JOURNAL OF MATERIALS SCIENCE **38** (2003) 4725–4733

Effects of grain size on the properties of a low nickel austenitic stainless steel

A. DI SCHINO
Materials Engineering Center, University of Perugia, Loc. Pentima Bassa 21, 05100 Terni, Italy

M. BARTERI
Centro Sviluppo Materiali, Via B. Brin, 05100 Terni, Italy

J. M. KENNY*
Materials Engineering Center, University of Perugia, Loc. Pentima Bassa 21, 05100 Terni, Italy
E-mail: kenny@unipg.it

The effect of the grain size (varying in the range of 2.5–50 μm) on the mechanical properties and on the wear and corrosion resistance of a low nickel austenitic stainless steel is reviewed. In particular, the austenite-martensite transformation followed by annealing for martensite reversion in high nitrogen stainless steel is investigated. In order to study the effect of this thermo-mechanical process on grain refinement, the effect of cold reduction, annealing temperature and annealing times were analysed. After obtaining ultrafine grains, the effect of the grain size on the hardness and the tensile properties was evaluated and showed a Petch-Hall dependency in the fully analysed range (down to a 2.5 μm grain size).

The fatigue behaviour of the steel is studied as a function of the grain size showing a poor influence of grain refining on the fatigue resistance. An increase of both the wear resistance and of the localized corrosion resistance with grain refining is also detected. Results are compared to those of similar measurements on a standard AISI 304 steel.

1. Introduction

Austenitic stainless steels have good corrosion resistance and good formability but they also have a relatively low yield strength. It is well known that the mechanical properties of austenitic stainless steels are very sensible to chemical composition (which can induce hardening by both a substitutional and interstitial solid solution) and to grain size [1, 2].

Recent developments in stainless steel have taken advantage of the changes in the chemical composition induced by nitrogen addition [3, 4] and showed that nitrogen alloyed austenitic stainless steels exhibit attractive properties such as high strength and ductility, good corrosion resistance and a reduced tendency of grain boundary sensitization. The high austenitizing potential of nitrogen allows the nickel content in the steel to be reduced, offering additional advantages such as cost saving. The production of these low nickel steels is made possible by the addition of manganese that allows an increase of the N solubility in the melt and decreases the tendency of Cr_2N formation [3].

Another effective way to increase yield strength without impairing ductility is grain refining. Since austenitic stainless steels do not undergo phase transformation at typical annealing temperatures, the only way to refine the grain is either by dynamic recrystallization, by imposing very severe deformations (uni-axial or multi-axial) [5] or by thermo-mechanical processes, including deformation or phase transformation [6]. It is well known that the transformation of austenite to martensite is the basic reaction in the hardening of carbon steel [7]. It is less well known, however, that this transformation may also play an important role in austenitic stainless steel. According to Cohen *et al*. [8] the martensitic transformation is a nucleation-and-shear process with strain embryos as starting points for the transformation. For martensite transformation, as for any other reaction, the following two conditions must be fulfilled:

- The free energy of the system must decrease during transformation;
- Nuclei must be present.

Cohen *et al*. [8] suggested that screw dislocations constitute nuclei for martensite formation. This was later proved by Krisement [9] in a theoretical study

*Author to whom all correspondence should be addressed.

on martensite transformation. As a result of the large number of dislocations that exist, even in a well annealed austenitic structure, more embryos than are necessary for the reaction to occur are generally present. The controlling factor for the kinetics of the transformation, therefore, is not the rate of nucleation but the supply of free energy. The free energy change of the system must be large enough to enable the reaction to mount an activation barrier between the austenitic and martensitic states. Since martensite does not form spontaneously at the thermodynamic equilibrium temperature, an undercooling of about 200–300°C is usually required. Angel [10] investigated this transformation in austenitic stainless steel and found that the amount of martensite increased with a decrease in the degree of cold working and decreased with an increase in the working temperature.

The research reported here has been carried out to analyse the effect of martensitic transformation and of the subsequent austenitic reversion on grain refining in a high nitrogen and low nickel austenitic stainless steel, thus combining both the nitrogen alloying and grain refining effects in order to obtain a highly resistant steel.

2. Materials and experimental details

The chemical composition of the low nickel stainless steel (hereinafter LNi), considered in this work, is shown in Table I. Industrial hot rolled and annealed samples (50 × 200 mm), whose thickness was 3 mm, were cold rolled using different thickness reductions (from 5% to 75%). The grain size before cold reduction was approximately 25 μm.

In order to analyse the effect of the cold rolling temperature on martensite formation, the following procedure was carried out: cold reduction was carried out at two different temperatures: in the former case, specimens were rolled after cooling in liquid nitrogen (about −100°C) and in the second, they were deformed without any prior cooling (at room temperature). In both cases, the martensite content was measured after deformation by a ferritoscope. The deformation and martensite content were considered homogeneous within the samples. Quenched and cold rolled samples were then annealed at different temperatures (in the range of 700°C to 1100°C), in order to investigate the martensite-austenite reversion. Samples were analysed after austenite reversion and automatic image analysis was used to measure the grain size.

Furthermore, in order to investigate the effect of the grain size on the mechanical properties of the steel, longitudinal ISO 50 tensile test specimens were cut from samples corresponding to different annealing conditions. Tensile tests were carried out with a deformation rate of 3 mm/min. The hardness of the steel was determined using a microhardness tester, equipped with a Vickers indenter at a load of 500 g.

The fatigue behaviour of the steel was studied as a function of the grain size. In particular, samples of LNI and AISI 304 (for comparison purposes) with grain sizes of 2.8 μm, 17.1 μm and 47.2 μm were tested for fatigue behaviour by means of a 160 kN servohydraulic testing machine applying an axial load. Tests were carried out under uni-axial sinusoidal loading at a frequency of 10 Hz up to 2×10^6 cycles.

In order to analyse the grain size effect on the corrosion resistance, steel materials were machined to corrosion test specimens of 15 × 15 × 1 mm. The specimen surface was polished by using increasingly finer abrasive papers, starting from 300 grit paper and finishing with 4000 grit paper. They were then immersed in different solutions and their corrosion was measured by their weight loss after the test. Potentiodynamic polarisation tests were carried out at 25°C in a conventional glass cell, using a deareated 35 g/1 NaC1 solution as electrolyte. The potential of the working electrode was measured using a saturated calomel electrode (SCE) as a reference. The counter electrode was a platinum foil and the scanning rate was 2.4 v/h. Before starting, a cathodic reduction of the passive film was performed at-1 V/SCE for 90 s. The pitting potential values, E_p, were taken as the last value at which the current was as low as that of a completely passive specimen. Each specimen was subjected to a minimum of three complete scans.

Cavitation resistance was measured by means of a vibratory test. This system uses a device to produce a high frequency (20 kHz) vibration in a test specimen immersed in a liquid. During half of each vibration cycle, a low pressure is created at the test specimen surface, producing cavitation bubbles. During the other half of the cycle, bubbles collapse at the specimen surface producing damage to the specimen and erosion thereof. Although the mechanism for generating fluid cavitation in this method differs from that occurring in flowing systems and hydraulic machines, the nature of the material damage mechanism is believed to be basically similar. The method therefore offers a small scale, relatively simple and controllable test that can be used to compare the cavitation erosion resistance of different materials and to study the nature and progress of damage in a given material in detail. Moreover, by varying some of the test conditions, the effect of test variables on the damage that occurs can be studied. This standard test procedure for ultrasonic cavitation testing has been approved by the American Society for Testing and Materials (ASTM) as Standard G 32 (ASTM 1992). The technique used here has been slightly modified by placing the test specimen a small distance below the tip of the ultrasonic probe.

TABLE I Chemical compositions of the studied stainless steels (mass, %)

	Cr	Ni	Mn	Si	Mo	N	C
LNI	16.5	1.07	11.4	0.12	1.0	0.30	0.037
AISI 304	18.4	8.6	1.50	0.61	0.06	0.024	0.06

3. Results and discussion

3.1. Microstructural evolution

The curves relating the martensite content M to the true strain ε, are shown in Fig. 1 for the cooled and deformed steel and for the steel deformed without prior cooling. In the cooled and deformed steel, an amount of

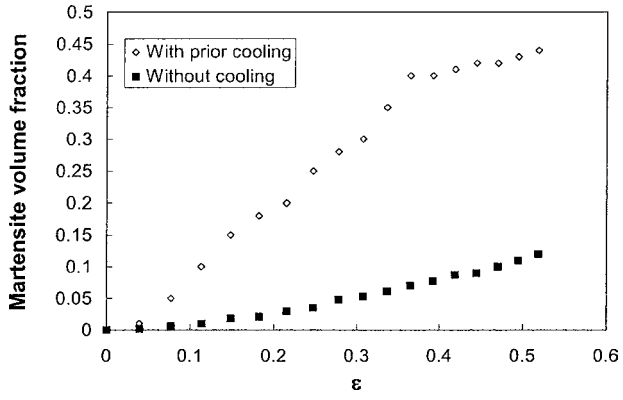

Figure 1 Formation of martensite by cold rolling with and without prior cooling in liquid nitrogen.

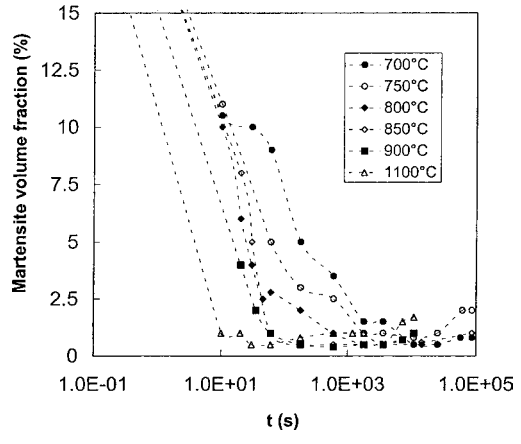

Figure 2 Effect of annealing time and temperature on the reversion behaviour of martensite.

about 45% of γ is transformed into martensite, using a 75% reduction ($\varepsilon = 0.52$) deformation ratio, while, in the steel rolled without cooling, only 12% martensite is produced after a 75% cold reduction. Results of similar measurements on a standard AISI 304 [11] showed that, at the same deformation ratio for this steel, about 80% martensite was obtained after cooling at -100°C and cold rolling. The lower martensite content in the high nitrogen steel is due to the addition of Mn and N that stabilize austenite against strain induced martensite formation. Only the sample deformed at 75% after cooling in liquid nitrogen was subjected to reversion treatment because grain refinement increases with an increase in martensite content [11].

In order to check the reversion kinetics, this sample was annealed at different temperatures (700°C to 1100°C) and times (10 s to 100 ks). Fig. 2 shows the evolution of the reversed martensite volume fraction as a function of annealing time and annealing temperature. The dotted lines connect the data to the initial martensite volume fraction (45%). It can be observed that, as expected, the martensite volume fraction decreases as time increases and the martensite reversion rate increases with an increase in the annealing temperature. Fig. 2 can be used to determine the martensite-austenite reversion kinetics for this material. The effect of annealing temperatures and times on the grain size is shown in Fig. 3. Results show that at 900°C, even for long annealing periods, no significant grain growth

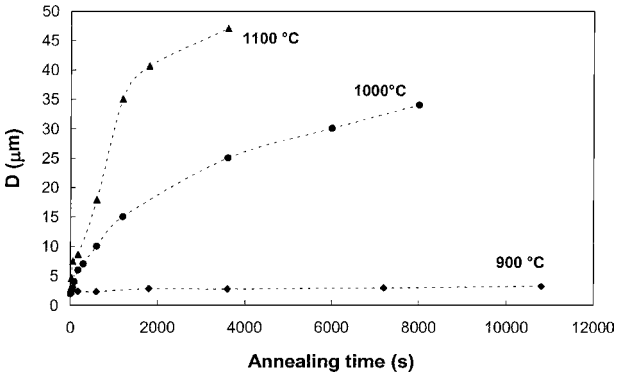

Figure 3 Effect of annealing temperatures and times on grain size.

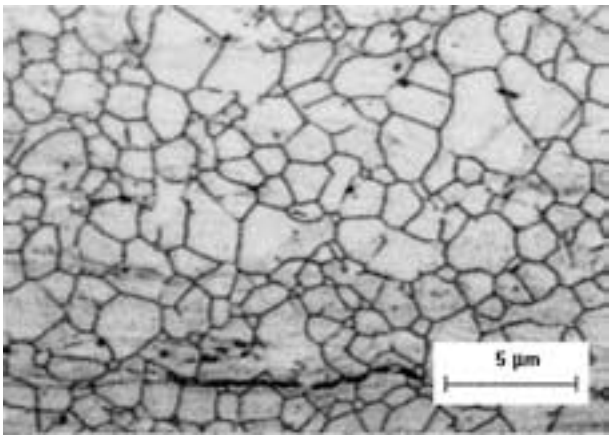

Figure 4 Microstructure of LNI steel annealed at 900°C for 600 s.

takes place. The grain size varies from 2.4 μm after 10 s annealing to 3 μm after 10 ks. Further measurements at lower annealing temperatures show that also in these cases the minimum obtainable grain size is about 2.4 μm. This can be explained assuming that the minimum austenite grain size depends on the number of nuclei per unit volume induced by deformation. Since all the samples come from the same cold rolled steel, they will have the same number of nuclei before annealing and so show the same recrystallized grain size. On the contrary, as expected, thermally activated grain growth occurs at $T = 1100$°C and grain size quickly increases. In Fig. 4, the microstructure of the sample annealed at 900°C for 600 s is shown, and in Fig. 5, its grain size distribution, measured by an automatic image analyzer, is shown.

3.2. Mechanical properties

Grain refinement is commonly known to increase the hardness and the strength of grained materials. It is well recognized that the yield stress R_{p02} and the hardness HV of a metallic material increase with decreasing grain size d. In particular, the Hall-Petch equation expresses the grain-size dependence of strength and micro hardness [10, 11]. In terms of strength and hardness, the Hall-Petch equations are:

$$R_{p02} = R^0_{p02} + kd^{-1/2} \quad (1)$$

$$H = H_0 + k'd^{-1/2} \quad (2)$$

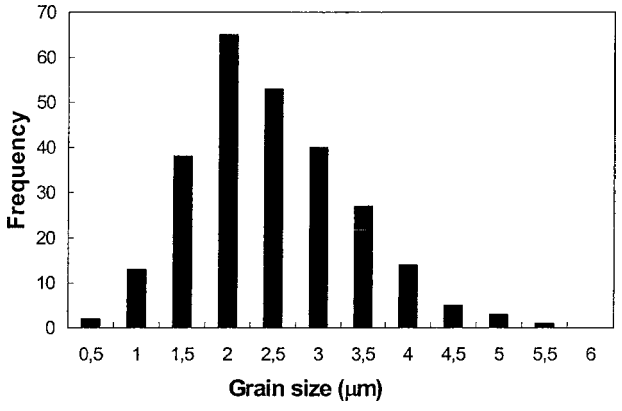

Figure 5 Grain size distribution of LNI steel annealed at 900°C for 600 s.

where the superscript 0 relates to the material of infinite grain size; k and k' are constants that represent the grain boundary as an obstacle to the propagation of deformation. The effect of grain size on tensile properties is shown in Figs 6 and 7, where similar measurements on a standard AISI 304 stainless steel are also reported. The positive effect of nitrogen addition in increasing steel strength for a given grain size is outlined and furthermore, the effect of grain size on strengthening is observed for both types of steel. In particular, the

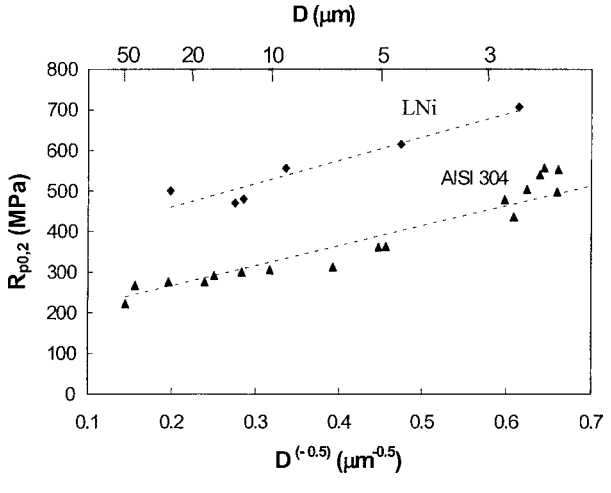

Figure 6 Dependency of yield strength on the grain size of high nitrogen and AISI 304 stainless steel.

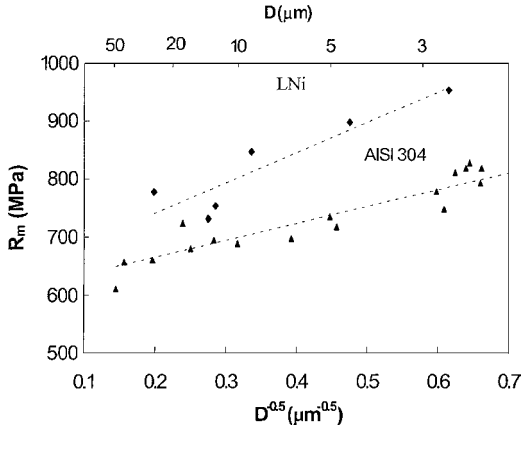

Figure 7 Dependency of tensile strength on the grain size of high nitrogen and AISI 304 stainless steel.

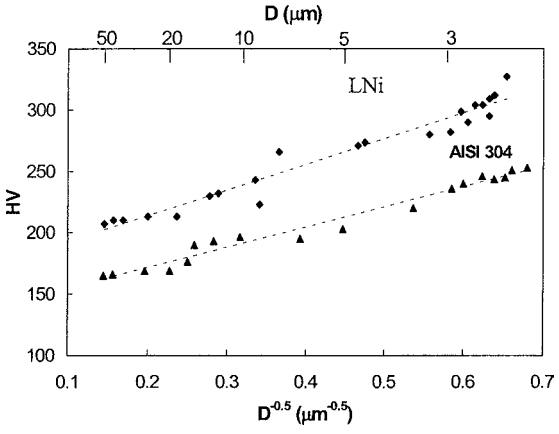

Figure 8 Dependency of hardness on the grain size of high nitrogen and AISI 304 stainless steel.

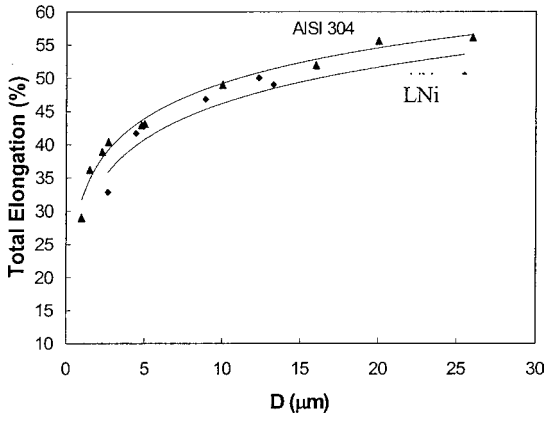

Figure 9 Grain refinement effect on the ductility of high nitrogen steel compared to AISI 304 stainless steel.

Hall-Petch dependency for both yield stress (R_{p02}) and tensile strength (R_m) is found to be valid for the examined grain size ranges for both high nitrogen steel and AISI 304 stainless steel. In Fig. 8, hardness versus the inverse square root of grain size is reported for both the high nitrogen and the AISI 304 stainless steel. Finally, Fig. 9 shows that the ductility of the high nitrogen steel is slightly lower than that of the AISI 304 stainless steel. Total elongation is reduced when grain size is refined in both types of steel.

3.3. Fatigue behaviour

In order to evaluate the effect of the grain size on the fatigue behaviour of the LNI steel, samples of high nitrogen steel in a cold rolled state were annealed at 1100°C for 20 s (sample A1), 3 min (sample A2) and 10 min (sample A3), in order to obtain three different austenitic microstructures with a 3.0 μm, 17.0 μm and 47.0 μm grain size, respectively. The fatigue resistance of the A1, A2 and A3 samples is reported in Fig. 10. The data shows that the influence of grain size on the fatigue behaviour of LNI steel is poor. Optical analysis showed that in LNI steel, small surface crack formation started early during cyclic straining but that nucleation ceased after approximately half of the life time. The mean crack length increased continuously until final failure. Crack initiation is related to the formation

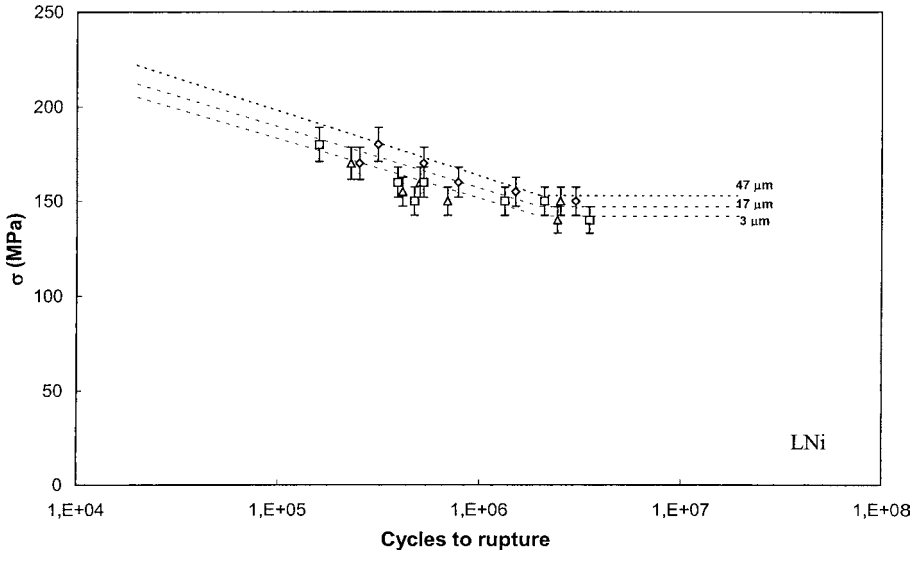

Figure 10 Grain size dependence of the fatigue resistance of LNI stainless steel.

of slip bands of the surface, which formation is promoted by nitrogen alloying [12]. A coarser grain size may cause a transition to inter-granular crack initiation. However, LNI steel cracks that grow exclusively in a transgranular manner independently of grain size were observed and consequently, the influence of grain size on fatigue behaviour is poor. Results of similar measurements performed on AISI 304 steel are reported in Fig. 11. A wider spread of data, as a function of grain size, is evident with respect to the LNI steel. In particular, an increase in fatigue resistance is found with decreasing grain size. A comparison between similar grained samples of LNI and AISI 304 steel are reported in Figs 12–14. In the case of samples A2 and A3, LNI steel shows a higher resistance with respect to AISI 304 steel. On the contrary, in the finest grained samples, the grain refining effect on the AISI 304 makes this steel more fatigue resistant with respect to LNI steel. In order to outline this effect better, a comparison between the stresses corresponding to 2×10^6 cycles in LNI and AISI 304 steel as a function of their grain sizes is reported in Fig. 15. The data shows how the beneficial effect of nitrogen alloying, in enhancing the fatigue behaviour of LNI steel with respect to the AISI 304, decreases with decreasing grain size, due to a strong improvement in the fatigue resistance of the latter steel.

3.4. Corrosion resistance

The general corrosion (GC) rate of the LNI stainless steel with grain sizes of 2.5 to 40 μm was measured in a 5% H_2SO_4 boiling solution for 36 ks, and the results are shown in Fig. 16. The corrosion rate of LNI steel increases with decreasing grain size. These results can be interpreted in terms of defects concentrated in the grain boundaries; so, increasing the grain boundary surface area by grain refining seems to cause passive film destabilization and thus ultrafine-grained steel shows a reduction of the general corrosion resistance. Furthermore, the GC rate of the LNI steel is higher than that of the standard AISI 304 steel. This can be explained in terms of the higher inclusion density in LNI with respect

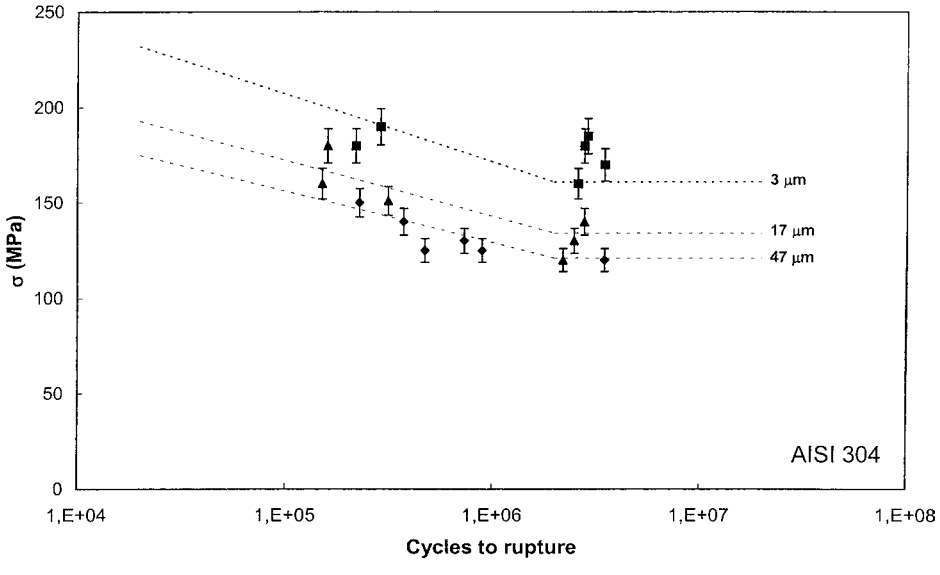

Figure 11 Grain size dependence of the fatigue resistance of AISI 304 stainless steel.

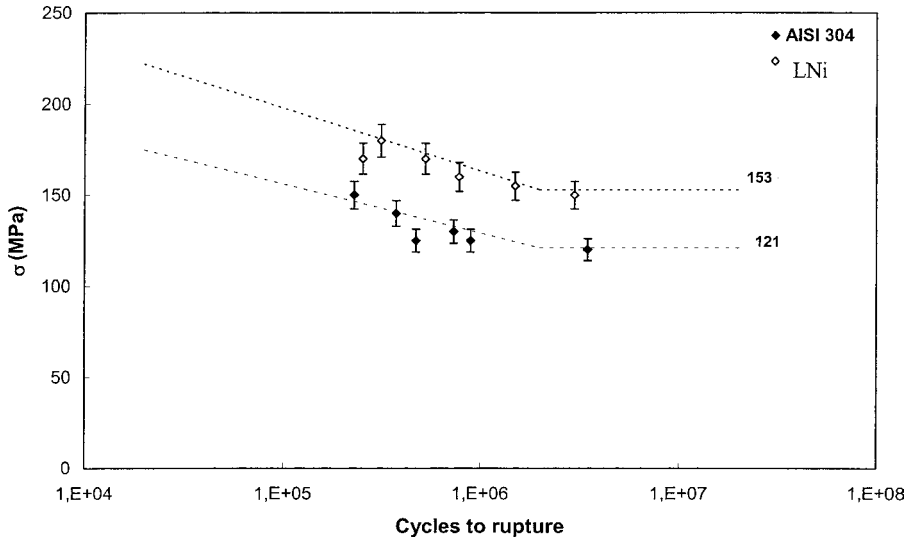

Figure 12 Fatigue resistance of the A3 LNI sample in comparison to a similar grained AISI 304 stainless steel.

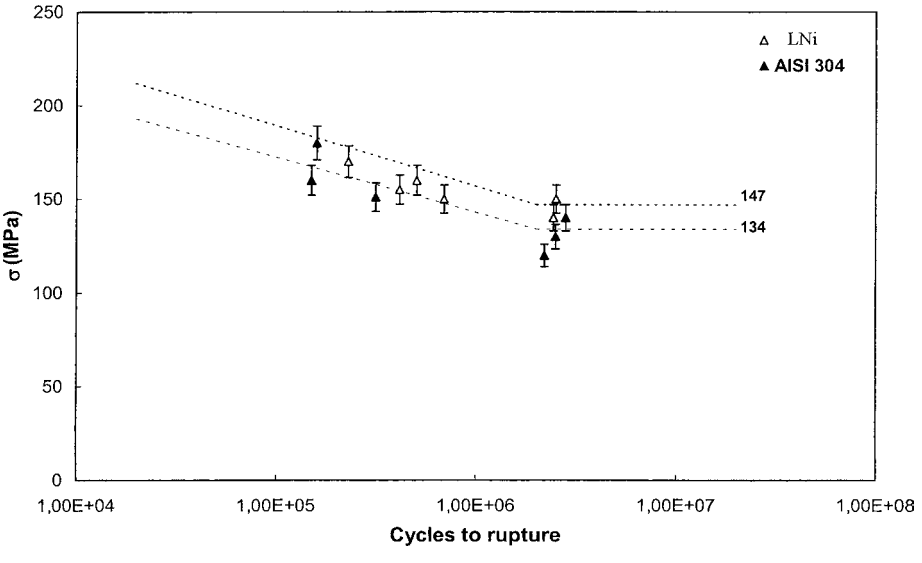

Figure 13 Fatigue resistance of the A2 LNI sample in comparison to a similar grained AISI 304 stainless steel.

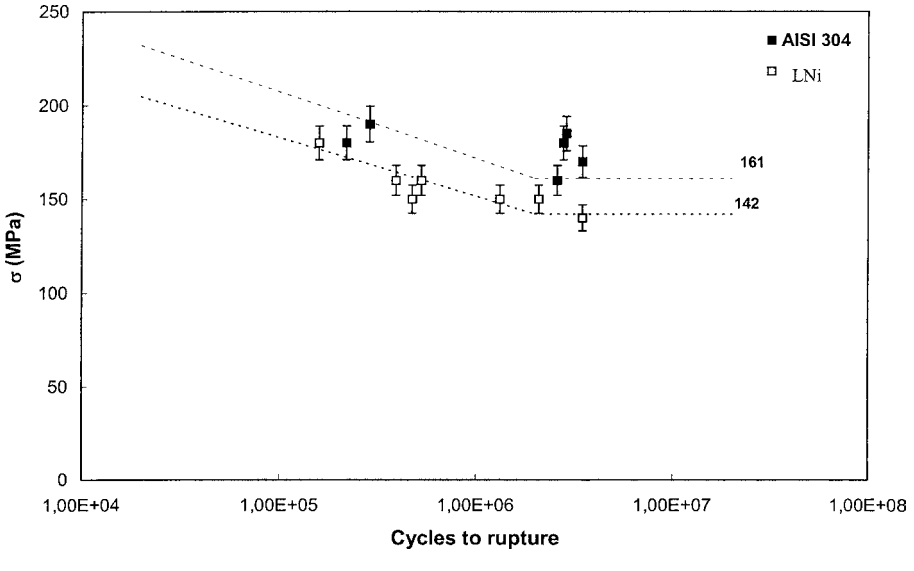

Figure 14 Fatigue resistance of the A1 LNI sample in comparison to a similar grained AISI 304 stainless steel.

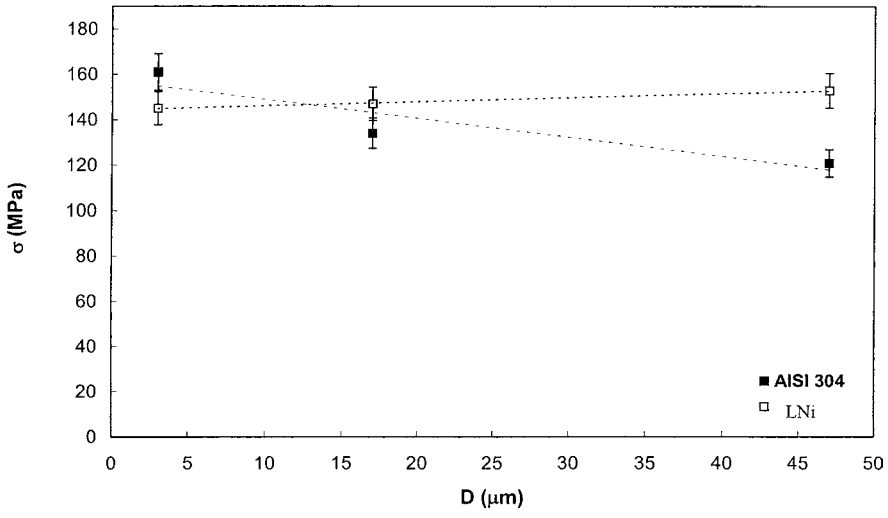

Figure 15 Comparison between the stresses corresponding to 2×10^6 cycles in LNI and AISI 304 steel as a function of their grain sizes.

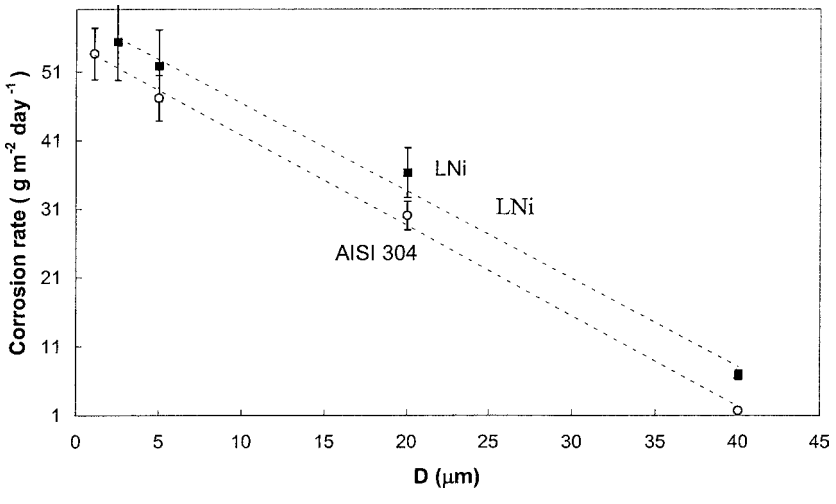

Figure 16 Relationship between the general corrosion rate in boiling 5% H_2SO_4 solution and the average grain size.

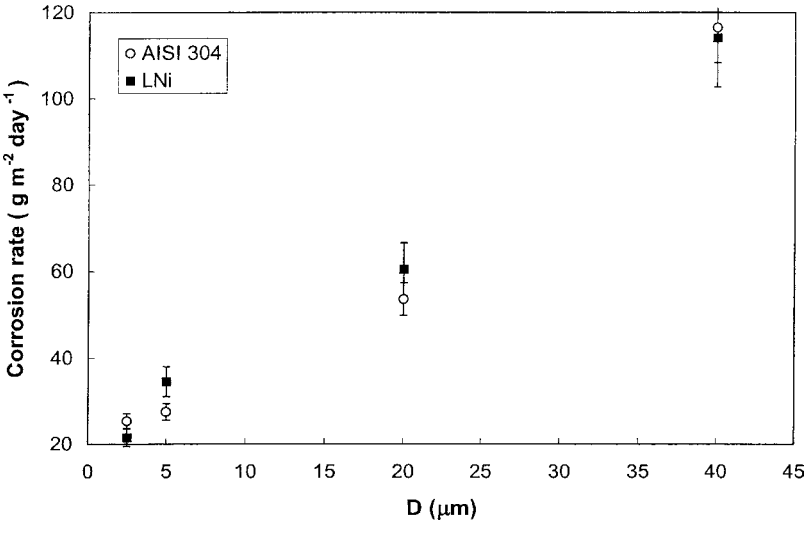

Figure 17 Relationship between the intergranular corrosion rate in a boiling Streicher solution and the average grain size.

to AISI 304 steel due to Mn alloying, as confirmed by an investigation with Scanning Electron Microscopy.

The intergranular corrosion rate (IGC) of LNI stainless steel was measured in H_2SO_4-$FeSO_4$ (Streicher solution) for 36 ks and the results are shown in Fig. 17. The corrosion rate decreases with decreasing grain size. As inter-granular corrosion is caused by the precipitation of carbides in the grain boundaries, the corrosion rate is affected by the volume fraction of precipitated carbides per unit of grain boundary area. As grain size is refined, the grain boundary areas per unit volume increase and the degree of the Cr depletion caused by

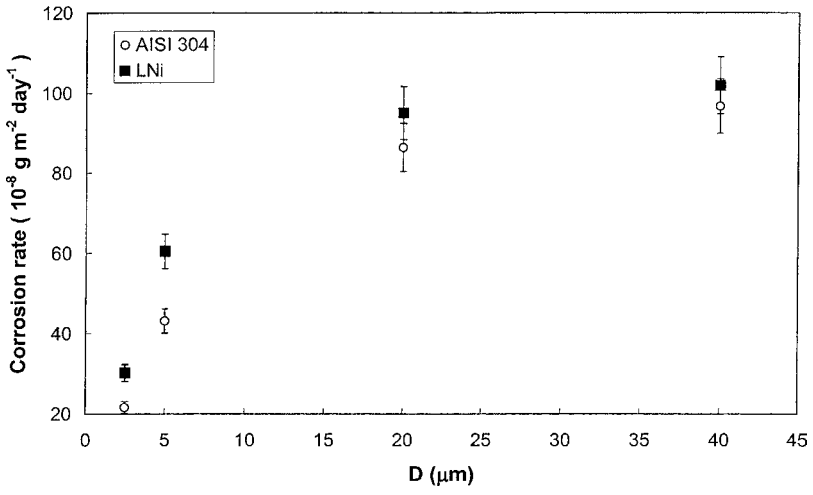

Figure 18 Relationship between the corrosion rate in a 10% $FeCl_3$-$6H_2O$ solution and the average grain size.

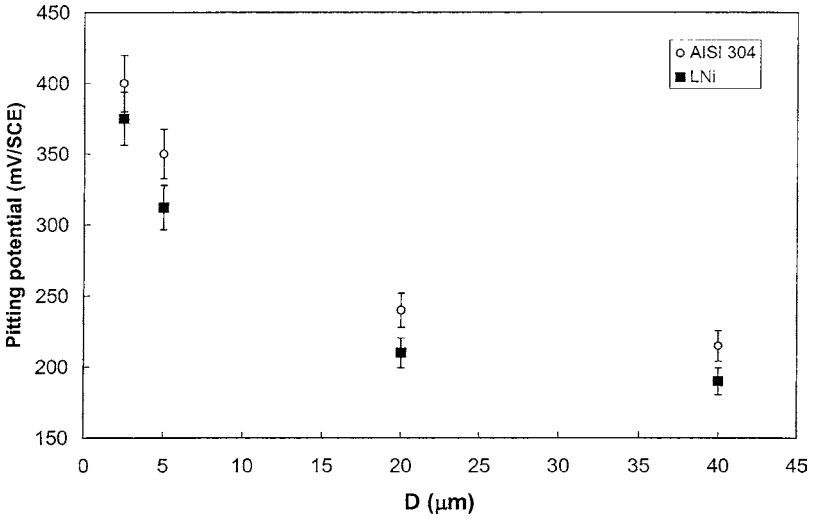

Figure 19 Relationship between the pitting potential E_p in a 3.5% NaCl solution at 303 K and the average grain size.

carbide precipitation decreases for a given C content. Hence, boundaries may not be sensitised in finely grained materials. Furthermore, the IGC rate of the LNI steel is comparable to that of the AISI 304 steel, the Cr and C contents being almost the same in both types of steel (see Table I).

The weight loss in a 10% $FeCl_3$-$6H_2O$ solution at room temperature for 36 ks and the results and comparison to standard AISI 304 steel are shown in Fig. 18. The corrosion resistance of the LNI steel in this solution is lower than that of the AISI 304 steel; also in this case, this result can be explained in terms of a higher inclusion density in the LNI steel with respect to the standard steel. Furthermore, in contrast with the reduction of the general corrosion resistance, grain refining leads to an improved corrosion resistance in both types of steel. The pitting of coarsely grained steel initiates in limited sites, with large and deep individual pits. In contrast, the pitting of ultrafine grained steel initiates in several sites, but with small individual pits revealed by microscopy, which results in a decreasing corrosion rate.

In order to evaluate the pitting corrosion resistance, potentiodynamic measurements have been carried out. Results, reported in Fig. 19, show that the pitting potential shifted towards more noble potentials with decreasing grain size.

Samples A1 and A3 were also tested for cavitation resistance. The cumulative volume loss due to cavitation corrosion for both samples is plotted as a function of cavitation time in Fig. 20. The material loss results show a distinctive behaviour as a function of cavitation time that can be divided into two stages: the first stage is characterized by an induction period during which very little material loss is detected and the second stage represents a steady-state erosion condition, where there is a constant rate of material removal from the surface of the eroded specimen. While induction time seems to be independent of grain dimension, different values of the cavitation rate, obtained from the slope of the curve in the steady-state erosion regime, were found: 0.06 and 0.10 g mm^{-2} h^{-1} for samples A1 and A3 respectively. The clearly beneficial effect of grain refining is evident. These results can be explained assuming that grain boundaries act to prevent flow due to a material build-up occurring at the grain boundaries. This conclusion agrees with the results reported by Pohl [13], who showed that in polycrystalline materials, even a low grain boundary surface density can provide a dominant supporting action against cavitation mechanisms. He

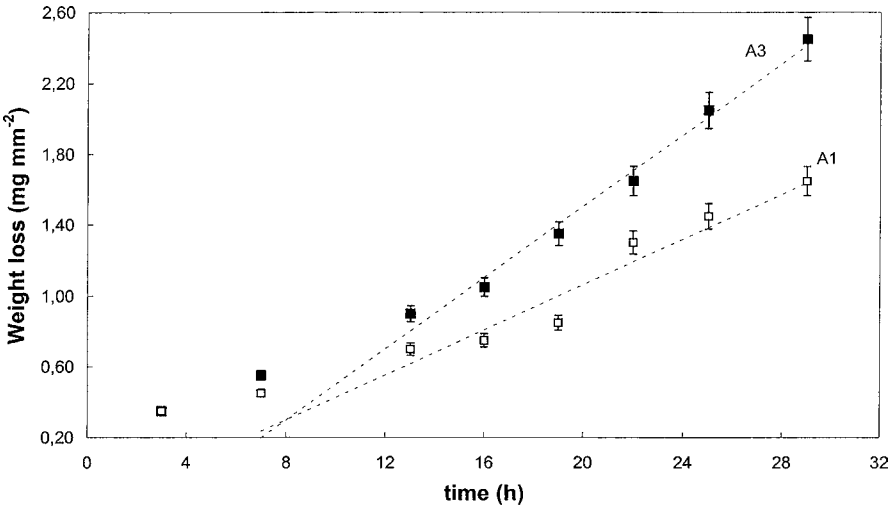

Figure 20 Results of the cavitation measurements of the LNI steel as a function of grain size.

showed further that in standard polycrystalline metals, the cavitation-erosion resistance continuosly increases with decreasing grain size.

4. Conclusions

In this paper grain refinement was applied to austenitic stainless steel with a high nitrogen content and the effect of grain size upon the mechanical and corrosion behaviour was examined. The following conclusions can be drawn out:

- The austenitic-martensite-austenitic transformation by deformation and annealing treatment resulted in steel with an average grain size as small as 2.5 μm.
- The mechanical characterization of austenitic steel with different grain sizes showed that the microhardness increases with decreasing grain size, as does the yield and flow stress. However a slight decrease in the ductility was also observed with decreasing grain size.
- Grain refining is found to have a poor effect on the fatigue behaviour of the high nitrogen austenitic stainless steel; this has been explained in terms of the formation of slip bands on the steel surface promoted by nitrogen alloying, with crack initiation related to this formation and independent of grain size. On the contrary, a strong beneficial effect of grain refining was detected in the fatigue behaviour of standard AISI 304 steel.
- From the corrosion tests, it can be drawn out that both the inter-granular and pitting corrosion rate decreases with decreasing grain size while the general corrosion resistance is impaired by grain refining.
- A beneficial effect of grain refining has been demonstrated in the high nitrogen austenitic stainless steel with reference to cavitation resistance and has been explained in terms of a material build-up at the steel grain boundaries.

Acknowledgements

The collaborations of *Swiss Center for Electronics and Microtechnology Inc*. (Switzerland) is gratefully acknowledged.

References

1. R. W. CAHN and P. HAASEN, "Physical Metallurgy" (Elsevier Science Publisher, 1983) p. 285.
2. A. DI SCHINO, J. M. KENNY and M. BARTERI, *Mater. Engin.* **11** (2000) 141.
3. A. RECHSTEINER and M. SPEIDEL, in Proc. of the 1st European Stainless Steel Conference, Florence, 1997, Vol. 2, p. 107.
4. A. DI SCHINO, J. M. KENNY, M. G. MECOZZI and M. BARTERI, *J. Mater. Sci.* **35** (2000) 4803.
5. S. S. HECKER, M. G. STOUT and J. L. SMITH, *Metall. Trans.* A **13** (1982) 619.
6. Y. MURATA, T. TAKEMOTO and Y. UEMATSU, in Proc. of the Int. Conference on Stainless Steels, Chiba, 1991, p. 510.
7. R. E. REED-HILL, "Physcial Metallurgy Principles" (PWS Publishing Company, 1994) p. 387.
8. M. COHEN, M. S. MACHLIN and V. G. PARANJPE, "Thermodynamics in Physical Metallurgy" (American Society for Metals, 1950) p. 264.
9. O. KRISEMENT, *Arch. Eisenh* **24** (1953) 191.
10. T. ANGEL, *J. Iron and Steel Inst.* (1954) 165.
11. A. DI SCHINO, I. SALVATORI and J. M. KENNY, *J. Mater. Sci.* **37** (2002) 4561.
12. J. O. NILSSON, *Scr. Metall.* **17** (1983) 593.
13. M. POHL, *Prakt. Metallog.* **33** (1996) 168.

Received 23 January
and accepted 29 July 2003